ACS APPLIED ENERGY MATERIALS

Letter

Cite This: ACS Appl. Energy Mater. 2019, 2, 3021−3027

www.acsaem.org

Phenothiazine-Based Hole-Transporting Materials toward Eco-friendly Perovskite Solar Cells

Jagadish Salunke,*[,†] Xing Guo,[‖] Zhenhua Lin,[‖] João R. Vale,[†,§] Nuno R. Candeias,[†] Mathias Nyman,[‡] Staffan Dahlström,[‡] Ronald Österbacka,[‡] Arri Priimagi,[†] Jingjing Chang,*[,‖] and Paola Vivo*[,†]

[†]Faculty of Engineering and Natural Sciences, Tampere University, P. O. Box 541, 33101 Tampere, Finland

[‡]Physics, Faculty of Science and Engineering and Center for Functional Materials, Åbo Akademi University, Porthansgatan 3, 20500 Turku, Finland

[§]Instituto de Investigação do Medicamento (iMed.ULisboa), Faculdade de Farmácia, Universidade de Lisboa, Avenida Professor Gama Pinto, 1649-003 Lisboa, Portugal

[‖]State Key Discipline Laboratory of Wide Band Gap Semiconductor Technology, Shaanxi Joint Key Laboratory of Graphene, School of Microelectronics, Xidian University, 2 South Taibai Road, Xi'an 710071, People's Republic of China

Supporting Information

ABSTRACT: Organic hole-transporting materials (HTMs), AZO-I and AZO-II, were synthesized via Schiff base chemistry by functionalizing a phenothiazine core with triarylamine(s) through azomethine bridges. Substantial enhancements in the power conversion efficiency (PCE = 12.6% and 14% for AZO-I and AZO-II, respectively) and stability (68% or 91% of PCE retained after 60 days for AZO-I or AZO-II, respectively) of perovskite solar cells (PSCs) were achieved when switching from mono- (AZO-I) to disubstituted (AZO-II) HTMs. The extremely low production costs (9 and 12 $/g for AZO-I and AZO-II, respectively), together with the Pd-catalyst-free synthesis, make these materials excellent candidates for low-cost and eco-friendly PSCs.

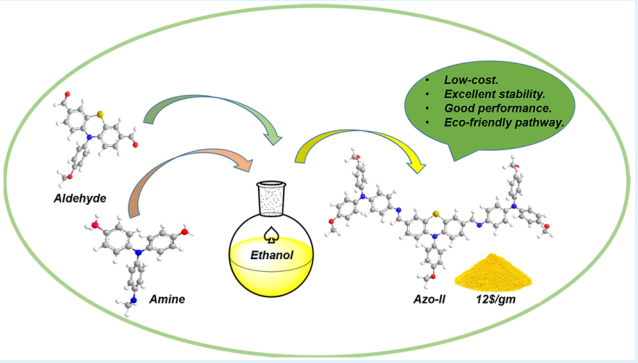

KEYWORDS: *phenothiazine, azomethine, hole-transporting materials, perovskite solar cells, eco-friendly, low-cost, stability*

Halide perovskite solar cells (PSCs) have recently received tremendous attention, due to their low-cost, high flexibility, low-temperature processing, and the skyrocketing rise of their power conversion efficiency (PCE), from 3.8% to 23.7%, in just less than a decade.[1,2] The excellent performance, together with the above-mentioned key features of PSCs, make them an attractive alternative to conventional photovoltaic technologies. PSCs consist of hole-transporting material (HTM), a light-absorbing layer (perovskite), and electron-transporting material (ETM), between two electrodes. The HTM layer plays a key role in PSCs as it facilitates the hole transfer from perovskite to the electrode and suppresses recombination, and also protects the perovskite surface against degradation due to moisture/oxygen.[3]

To date, most high-performance PSCs are based on either small molecular 2,2′,7,7′-tetrakis(*N*,*N*-di-*p*-methoxyphenylamine)-9,9′-spirobifluorene (spiro-OMeTAD) or polymeric poly[bis(4-phenyl)(2,4,6-trimethylphenyl)amine] (PTAA) HTM.[3] However, these materials are tremendously pricey (91.67 $/g (raw material cost)[4] and 2190 $/g (retail price)[5] for spiro-OMeTAD and PTAA, respectively) and also have major drawbacks such as low hole mobility, complex multistep synthesis, and difficult purification.[3] Thus, small-molecule HTMs based on pyrene,[6] carbazole,[7] phenothiazine,[8,9] dissymmetric fluorene−dithiophene (FDT),[10] fluorene terminated molecules,[14] and several others have been proposed as alternatives to spiro-OMeTAD.[3]

Almost all of the above-mentioned HTMs are synthesized in modest overall yields by means of toxic and expensive palladium-catalyzed cross-coupling reactions. The required stringent conditions and purification, hampers their low-cost large-scale production.[11] In addition, the presence of catalyst traces can prevent batch-to-batch reproducibility of solar cell performance.[12] Hence, designing simple, low-cost, and environmentally friendly HTMs, with high mobility and good stability, would be highly important toward commercialization of PSCs. Green HTMs based on, e.g., azomethine,[4] enamine,[13] hydrazone,[14] amide,[15] and aniline,[16] with good solar cell performance, have been reported.

Received: February 27, 2019
Accepted: April 8, 2019
Published: April 8, 2019

DOI: 10.1021/acsaem.9b00408
ACS Appl. Energy Mater. 2019, 2, 3021−3027

Scheme 1. Molecular Design and Synthetic Route for AZO-I and AZO-II

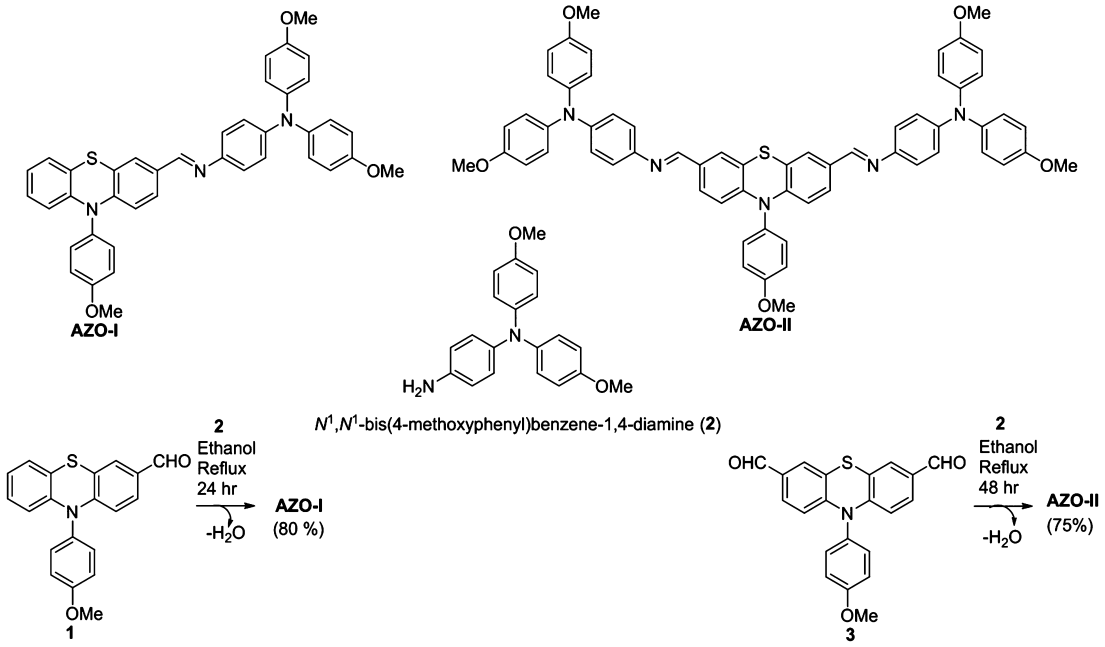

In particular, Docampo et al. have reported an azomethine-based 3,4-ethylenedioxythiophene (EDOT) core HTM EDOT-OMeTPA, demonstrating that Schiff base condensation chemistry is a viable route to achieve low-cost HTMs for high-performance PSCs, with reduced environmental impact.[4] In their design, EDOT was used as the central core, which, even if providing good performance, requires the use of chlorinated solvents, inert atmosphere, and acidic conditions for HTM synthesis. Moreover, the EDOT core presents additional challenges regarding solubility of the HTM and less freedom for functionalization, limiting the development of its soluble derivatives. To address these drawbacks, there is a need for combining the attractive azomethine-based chemistry with other cores.

Phenothiazine is a well-known electron-rich heterocycle, which has been extensively used in the context of organic transistors,[17] photovoltaics,[18] and light emitting diodes.[19] Recently phenothiazine has also proven to be an excellent building block for high-performing and cost-effective HTM in PSCs.[8,9] Its potential benefits are numerous. Phenothiazine is a cheap building block that possesses several possibilities for further functionalization. It is chemically stable and can exhibit very high hole mobilities.[20] It is also well-soluble in common organic solvents and has good film-forming properties. For all these reasons, we foresee phenothiazine as a particularly promising core unit for designing low-cost, environmentally friendly HTMs for high-performance PSCs.

Herein, we report on two new phenothiazine-based HTMs functionalized with azomethine moieties, AZO-I and AZO-II, shown in Scheme 1. Both materials are synthesized in excellent yields from cheap and readily available precursors, via a simple Pd-free synthetic route with only water as byproduct. To the best of our knowledge, AZO-I and AZO-II are among the cheapest phenothiazine core HTMs reported, amounting to 9 and 12 $/g, respectively (see the Supporting Information (SI) for details). Compared to the ubiquitous spiro-OMeTAD (raw material cost 91.67 $/g), these compounds provide a significant gain in cost and a greener synthesis pathway. When employed in PSCs, disubstitution of dimethoxy triarylamine groups yields improved properties as compared to monosubstitution in terms of both PCE and stability, the average PCEs being 12.6%, 14.0%, and 18.1% for AZO-I-, AZO-II-, and spiro-OMeTAD-based devices, respectively. Moreover, the devices comprising AZO-II were markedly stable, maintaining >90% of the PCE even after 2 months of storage of unencapsulated devices in ambient conditions with 30% relative humidity (RH).

The molecular design for AZO-I and AZO-II was inspired by the work of Docampo et al. on low-cost azomethine-based HTMs,[4] as well as the recent breakthroughs on phenothiazine-based HTMs.[8,9] We would especially like to mention the HTMs PTZ2 and Z30, reported by Abate and co-workers[8] and the Grätzel group,[9] respectively (see SI Figure S1 for the chemical structures of PTZ2 and Z30). Both PTZ2 and Z30 are very similar in molecular design to that of AZO-II, and they yield PCEs comparable to spiro-OMeTAD in PSC devices. However, they have been synthesized in modest overall yields (24.9% and 27.7% for PTZ2 and Z30, respectively) via multistep Pd-catalyzed Suzuki coupling reactions with challenging purification steps, rendering them relatively costly. In contrast, syntheses of AZO-I and AZO-II are straightforward, Pd-free, and significantly more efficient with overall yields of 51% (AZO-I) and 40% (AZO-II), as detailed further in the Supporting Information. Table S1 presents comparative details between the previously studied HTMs relevant for this study (EDOT-OMeTPA, PTZ2, Z30, and spiro-OMeTAD) and HTMs AZO-I and AZO-II. We note that methoxy-substituted triarylamine units are introduced to the phenothiazine core to increase the solubility, fine-tune the energy levels of the HTMs well-aligned to perovskite valence band, and ultimately boost the solar cell efficiency.[4]

To evaluate the applicability of these organic semiconductors in PSCs, we investigated the natural bond orbital (NBO) analysis of the optimized geometries of the azomethine compounds calculated with density functional theory (DFT) at PBE1PBE/6-31G**, followed by time-dependent calculations

DOI: 10.1021/acsaem.9b00408
ACS Appl. Energy Mater. 2019, 2, 3021−3027

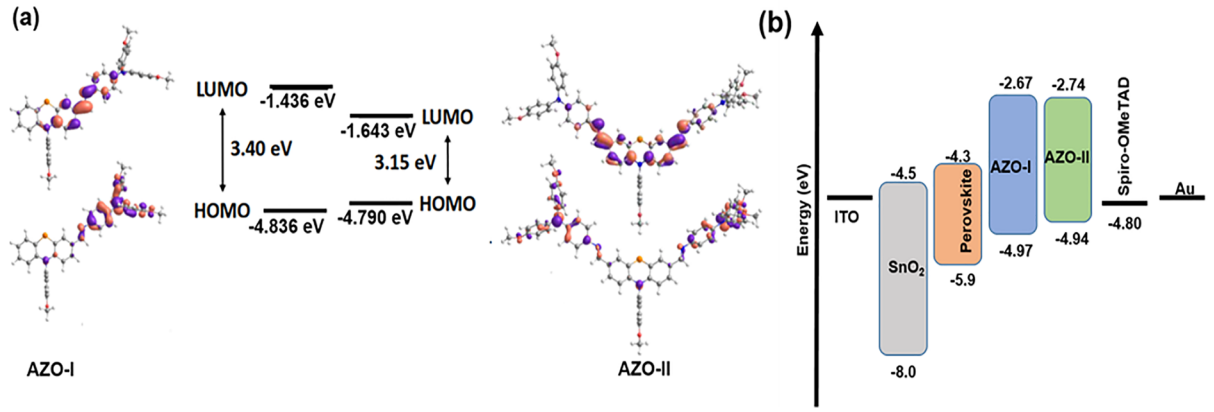

Figure 1. (a) Energy levels and electron distribution for frontier molecular orbitals of AZO-I and AZO-II calculated with DFT at PBE1PBE/6-31G** level of theory (isosurface value = 0.04). Energy values are presented in italics (eV). Details in SI and Figure S2. (b) Energy level diagram, as determined experimentally with DPV, for the HTMs used in PSC devices in this work.

Table 1. Optical, Electrochemical, Thermal Characterization, and Hole Mobility of AZO-I and AZO-II HTMs

	λ_{max} (nm) Abs/Emi								
HTM	DCM	Film	HOMO (eV)	LUMO (eV)	E_g (eV)	T_d (°C)	T_g (°C)	T_m (°C)	μ ($cm^2\ V^{-1}\ s^{-1}$)
AZO-I	422/534	430/544	−4.97[a], −4.83[b]	−1.43[b]	2.30[c], 3.40[b]	392	85	232	2×10^{-6}
AZO-II	453/548	460/554	−4.94[a], −4.79[b]	−1.64[b]	2.20[c], 3.15[b]	405	120	288	2×10^{-5}

[a]HOMO level determined by DPV. [b]Energy levels and E_g determined by TDDFT analysis. [c]E_g determined from optical bandgap.

(Figure 1a, Table S2). For AZO-II, the conjugation length is increased due to the disubstitution of dimethoxytriarylamine as compared to the monosubstitution in AZO-I, which is anticipated to lead to the enhancement of hole transport in AZO-II through the hopping mechanism.[21] The electron density of the HOMO level for both HTMs is located on the peripheral electron-rich dimethoxytriarylamine moieties, while the LUMO is spread over the phenothiazine unit including the electron-withdrawing azomethine bridge between the phenothiazine core and the triarylamine(s).[22,4] The calculated HOMO and LUMO energy levels are −4.84 and −1.44 eV for AZO-I and −4.79 and −1.64 eV for AZO-II (see Figure 1b). The small increase in HOMO level of AZO-II with respect to AZO-I can be ascribed to the slightly extended conjugation length in AZO-II due to the presence of two azomethine bridges.[23]

The absorption and emisssion spectra of the HTMs were measured in solution (1.0×10^{-5} M dichloromethane (DCM); Figure S4a) and in solid state (spin-coated films; Figure S4b). AZO-I and AZO-II show absorption maxima (λ_{max}) at 422/430 nm and 453/460 nm in solution/solid state, respectively, coresponding to the intramolecular charge transfer (ICT) of the $\pi-\pi^*$ transition.[24] The red shift of λ_{max} for AZO-II with respect to AZO-I can be ascribed to the more extended conjugation. The absorption onsets are 538 nm (AZO-I) and 555 nm (AZO-II), and the corresponding optical bandgaps, 2.3 and 2.2 eV, respectively, also in line with the more extended conjugation of AZO-II.[18] The photoluminescene maxima were at 534 nm (solution) and 544 nm (solid) for AZO-I and 548 nm (solution) and 554 nm (solid) for AZO-II (Figure S4).

The experimental determination of the energy levels was carried out through differential pulse voltammetery (DPV; Figure S5). The data are presented in Figure 1b and summarized in Table 1. The obtained HOMO levels of AZO-I and AZO-II are −4.97 and −4.94 eV, respectively, following a trend similar to those achieved by DFT calculations. The experimental HOMO level for spiro-OMeTAD in similar conditions was determined to be −4.80 eV (Figure S5). The relatively small energy difference in the HOMO levels as compared to spiro-OMeTAD (0.17 and 0.14 eV for AZO-I and AZO-II, respectively) indicates their potential applicability in PSCs based on mixed cation and halide perovskites ($Cs_{0.05}MA_{1-y}FA_yPbI_{3-x}Cl_x$), whose valence band is located at 5.9 eV.

The decomposition temperatures, corresponding to 5% weight loss (T_d) for AZO-I and AZO-II are 392 and 405 °C, respectively, as determined by thermogravimetric analysis (TGA; Figure S6 and Table 1), comparable to spiro-OMeTAD (424 °C). The glass transition temperatures (T_g) and the melting temperatures (T_m) were measured with differential scanning calorimetry (DSC; Figure S6). It was found that AZO-I showed T_g at 85 °C and T_m at 232 °C, whereas AZO-II exhibits T_g at 120 °C and T_m at 288 °C. We attribute the higher T_g/T_m of the latter to its larger molecular weight and stiffness.[9] Note also that the T_g of AZO-II is comparable to those of spiro-OMeTAD (120 °C) and the previously reported phenothiazine-based HTM Z30 (125.7 °C), which is important for the stability of the PSC devices.[4] The bulk hole mobility of the pristine HTMs was determined by integral mode time-of-flight (Q-TOF) method (Figure S7 and related discussion). The obtained hole mobilities for AZO-I and AZO-II are 2×10^{-6} $cm^2/(V\ s)$ and 2×10^{-5} $cm^2/(V\ s)$, respectively (Figure S7, Table 1). The fact that AZO-II displays 1 order of magnitude higher mobility than AZO-I can be attributed to the introduction of two electron-donating triarylamine groups in the 3,7-positions of the electron-rich phenothiazine core.[25] As a reference, under identical experimental conditions the mobility of spiro-OMeTAD (6×10^{-5} $cm^2/(V\ s)$; Figure S7) is comparable, though somewhat higher, than for AZO-II.

We also carried out steady-state photoluminescence (PL) and time-resolved photoluminescence (TR-PL) analysis to

DOI: 10.1021/acsaem.9b00408
ACS Appl. Energy Mater. 2019, 2, 3021−3027

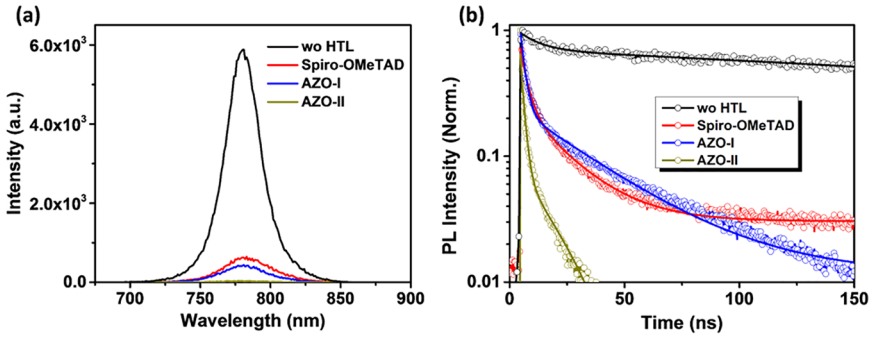

Figure 2. (a) Steady-state and (b) time-resolved photoluminescence spectra of spiro-OMeTAD, AZO-I, and AZO-II deposited on perovskites.

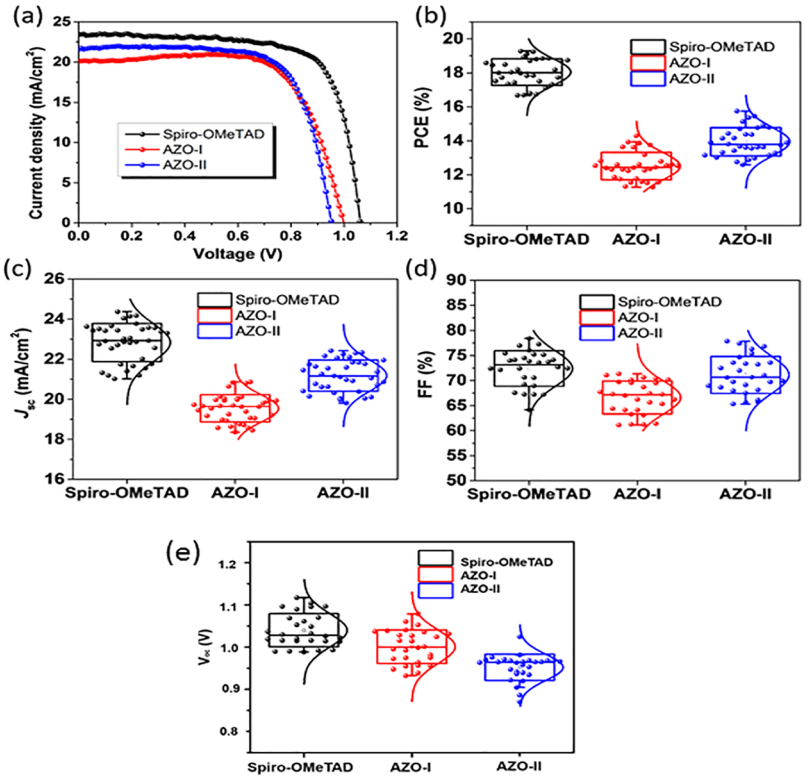

Figure 3. (a) Current density−voltage (J−V) curves for perovskite solar cells (reverse scans) measured with scan rate of 10 mV/s under AM 1.5G simulated solar light illumination by using spiro-OMeTAD, AZO-I, and AZO-II as HTMs. PCE (b), J_{SC} (c), FF (d), and V_{oc} (e) distributions of PSC devices based on different HTMs.

understand the charge extraction process at the perovskite/HTM interface. As shown in Figure 2a, when films of spiro-OMeTAD, AZO-I, or AZO-II were deposited on perovskite surface, the steady-state photoluminescence of the perovskite layer was quenched severely, as expected. The PL intensity of AZO-II was much lower than that of spiro-OMeTAD and AZO-I, suggesting that AZO-II could more efficiently extract the photogenerated holes from the perovskite layer. The higher quenching efficiency of AZO-II compared to AZO-I could be attributed to better film conductivity and enhanced charge transfer from perovskite to HTM. The TR-PL measurement was used to further analyze the hole-extraction process, as shown in Figure 2b. The carrier lifetimes were obtained by fitting the TR-PL curves with a double-exponential decay model presented in Table S6. The significantly faster decay of AZO-II allows us to conclude that the hole injection process from the valence band of perovskite to the HOMO level of the HTM is more efficient as compared to both AZO-I and spiro-OMeTAD. This is also consistent with the steady-state PL results (see in SI and Table S5).

In order to investigate the performance AZO-I and AZO-II in PSC devices and compare them to spiro-OMeTAD, we fabricated mixed cation and halide PSC devices (ITO/SnO_2/$Cs_{0.05}MA_{1-y}FA_yPbI_{3-x}Cl_x$/HTM/Au; see device fabrication details in the SI). The perovskite film quality was evaluated by field emission scanning electron microscope (FESEM) and X-ray powder diffraction (XRD) techniques (see Figure S8). As shown in Figure S8, the perovskite film exhibited a smooth and dense polycrystalline surface with large grain size (800−1200 nm). The XRD spectrum of the perovskite film further confirmed that good crystallinity was achieved. Current density−voltage (J−V) curves of the PSC devices employing the three HTMs, collected under simulated illumination (AM 1.5G, 100 mW cm^{-2}), are presented in Figure 3, and the photovoltaic parameters are summarized in Table 2. The HTMs were first employed in pristine form, with the aim of

DOI: 10.1021/acsaem.9b00408
ACS Appl. Energy Mater. 2019, 2, 3021−3027

Table 2. Photovoltaic Parameters Obtained from *J*−*V* Curves Based on Different HTMs

HTM	J_{SC} (mA/cm^2)	V_{oc} (V)	FF (%)	PCE (%)	PCE$_{max}$ (%)
AZO-I	20.1	1.00	66	12.6	14.3
AZO-II	21.6	0.95	71	14.0	15.6
spiro-OMeTAD	23.4	1.04	74	18.1	19.3

fabricating dopant-free PSC devices. However, due to the poor performance of devices based on undoped HTMs (Table S3), we used conventional Li- and Co-based dopants and made doped PSCs (see device fabrication details in the SI). The thicknesses of the HTMs were also optimized by using different solution concentrations. The devices based on AZO-I, AZO-II, and spiro-OMeTAD produced averaged short-circuit current densities (J_{SC}) of 20.1, 21.6, and 23.4 mA cm^{-2}, open-circuit voltages (V_{oc}) of 1.00, 0.95, and 1.04 V, and fill factors (FFs) of 0.66, 0.71, and 0.74, resulting in average PCEs of 12.6%, 14.0% and 18.1%, respectively (Table 2). The PCEs of champion devices based on AZO-I and AZO-II HTMs are 14.3% and 15.6%, respectively.

The poorer performance of AZO-I compared to the other two HTMs can be partly attributed to its lower hole mobility (2×10^{-6} cm^2 V^{-1} s^{-1}) compared to those of AZO-II (2×10^{-5} cm^2 V^{-1} s^{-1}) and spiro-OMeTAD (6×10^{-5} cm^2 V^{-1} s^{-1}).[26,27] Even though AZO-II showed better hole injection compared to spiro-OMeTAD based on the TR-PL quenching data, its lower performance in solar cells can be related to the lower J_{SC}, most likely due to its lower HOMO level.[28,29] The low HOMO level of AZO-I was beneficial for a larger built-in field for charge extraction/collection, resulting in larger V_{oc} compared to that of AZO-II. However, for both HTMs the V_{oc} values are smaller than that for spiro-OMeTAD-based devices, which may be caused by charge-recombination-induced voltage loss.[30] The higher J_{SC} and FFs of AZO-II-based devices compared to AZO-I can be ascribed to its higher hole mobility, responsible for efficient charge extraction and hole transport. All of the devices showed good reproducibility, as evident from the distribution of the photovoltaic data depicted in Figure 3.

To provide further insights into the interaction between perovskite and AZO-I/AZO-II in comparison to spiro-OMeTAD, we recorded *J*−*V* forward scans to evaluate the hysteresis (Figure S9) and measured the EQE spectra (Figure S10). Devices including AZO-I show the largest hysteresis, thus confirming the worst interaction with perovskite with respect to cells based on spiro-OMeTAD and AZO-II. On the other hand, the *J*−*V* characteristics of solar cells employing spiro-OMeTAD or AZO-II display a similar hysteresis behavior. The EQE spectra (Figure S10) of AZO-I and AZO-II devices show a sudden drop in the EQE around the absorption maxima wavelengths of the materials. With bandgaps around 2.2 eV, both AZO-I and AZO-II, may absorb a significant amount of light, thus partially justifying a detrimental effect on J_{SC} with respect to spiro-OMeTAD cells. However, the reduced performance of AZO-I-/AZO-II-based devices should be mostly related to HOMO level alignment (discussed above) and HTMs' conductivity issues, since the HTMs do not contribute to the EQE spectra as does the key light harvesting layer, the perovskite itself.

Finally, the unencapsulated devices based on spiro-OMeTAD, AZO-I, and AZO-II HTMs were stored in ambient conditions with ∼30% RH to evaluate their temporal stability, as shown in Figure 4. The devices based on AZO-II displayed

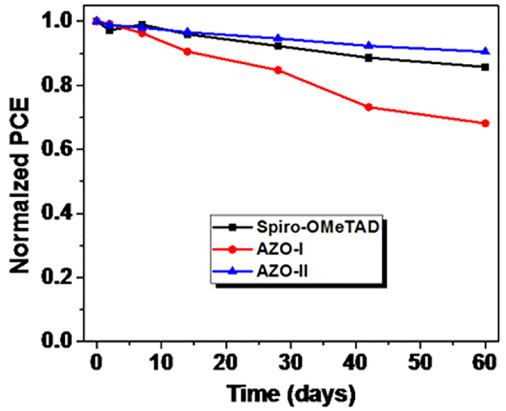

Figure 4. Long-time stability of the devices based on spiro-OMeTAD, AZO-I, and AZO-II as HTM.

remarkably long lifetimes over a prolonged time period. In fact, after 60 days, the devices based on AZO-II retained 91% of their initial PCE, while those employing spiro-OMeTAD and AZO-I retained 86% and 68%, respectively. These values are averaged from 15 independent devices. The poor performance of the devices based on AZO-I might also partly be caused by reduced encapsulation due to its lower thickness that minimizes the device series resistance (see the experimental details in the SI), together with its lower T_g.[12] The stability results further underpin that AZO-II, or more generally the materials design concept combining phenothiazine core and azomethine bridging, is promising for fabricating low-cost, eco-friendly, and high-performance HTMs for PSCs.

In conclusion, we designed and synthesized two phenothiazine-based HTMs, AZO-I and AZO-II, using simple, eco-friendly, and low-cost Schiff base chemistry and inexpensive precursors. When employed in PSC devices, AZO-II afforded an average PCE of 14.0% with excellent stability, maintaining >90% of the PCE even after 2 months' storage in ambient conditions with ∼30% RH. In addition to the relatively high performance, the production cost of AZO-II is extremely low, only 12 $/g. Given the low price and high stability, AZO-II, in spite of a small loss in the overall PSC performance as compared to that of spiro-OMeTAD-based reference devices (18.1% average PCE), is rather competitive with respect to state-of-the-art HTMs, demonstrating that phenothiazine-based low-cost derivatives synthesized by Schiff base chemistry hold a great potential for eco-friendly HTMs with minimal environmental impact. Further modification of the phenothiazine core can be conducted via N-substitution, in order to tune the energy levels, improve solubility in green solvents, and enhance the charge-carrier mobility, while retaining the low cost of production, hence paving the way toward green, phenothiazine-based PSCs with ever-improving performance.

■ ASSOCIATED CONTENT

Supporting Information

The Supporting Information is available free of charge on the ACS Publications website at DOI: 10.1021/acsaem.9b00408.

Details on synthetic procedures, DFT calculations, device fabrication procedures, hysteresis *J*−*V* scans, EQE spectra, fundamental characterization of all new

DOI: 10.1021/acsaem.9b00408
ACS Appl. Energy Mater. 2019, 2, 3021−3027

compounds, energy level calculations from differential pulse voltammetry, and cost analysis of the HTMs (PDF)

AUTHOR INFORMATION

Corresponding Authors

*(J.S.) E-mail: jagadish.salunke@tuni.fi.
*(J.C.) E-mail: jjingchang@xidian.edu.cn.
*(P.V.) E-mail: paola.vivo@tuni.fi.

ORCID

Jagadish Salunke: 0000-0002-7075-8066
Nuno R. Candeias: 0000-0003-2414-9064
Mathias Nyman: 0000-0002-1250-7111
Ronald Österbacka: 0000-0003-0656-2592
Arri Priimagi: 0000-0002-5945-9671
Jingjing Chang: 0000-0003-3773-182X
Paola Vivo: 0000-0003-2872-6922

Notes

The authors declare no competing financial interest.

ACKNOWLEDGMENTS

We thank Dr. Maning Liu for fruitful discussions and Mr. Arto Hiltunen for helping with the TGA measurements. J.S. is grateful to the Fortum Foundation (Grant 201800260) for funding. P.V., M.N., and R.Ö. acknowledge the Jane & Aatos Erkko Foundation (Project "ASPIRE"), and A.P. the Academy of Finland (Decision No. 311142), for financial support. This work is part of the Academy of Finland Flagship Programme, Photonics Research and Innovation (PREIN), Decision No. 320165.

REFERENCES

(1) Jena, A.; Kulkarni, A.; Miyasaka, T. Halide perovskite photovoltaics status, and future prospects. *Chem. Rev.* **2019**, *119*, 3036−3103.

(2) NREL. Best Research-Cell Efficiency Chart; https://www.nrel.gov/pv/assets/pdfs/best-reserch-cell-efficiencies.20190327.pdf, accessed: Mar. 27, 2019.

(3) Vivo, P.; Salunke, J. K.; Priimagi, A. Hole-Transporting Materials for Printable Perovskite Solar Cells. *Materials* **2017**, *10* (9), 1087.

(4) Petrus, M. L.; Bein, T.; Dingemans, T. J.; Docampo, P. A low cost azomethine-based hole transporting material for perovskite photovoltaics. *J. Mater. Chem. A* **2015**, *3*, 12159−12162.

(5) Sigma Aldrich.https://www.sigmaaldrich.com/technical-service-home/product-catalog.html, retrieved on Feb. 26, 2019.

(6) Jeon, N. J.; Lee, J.; Noh, J. H.; Nazeeruddin, M. K.; Grätzel, M.; Seok, S. Il Efficient Inorganic−Organic Hybrid Perovskite Solar Cells Based on Pyrene Arylamine Derivatives as Hole-Transporting Materials. *J. Am. Chem. Soc.* **2013**, *135*, 19087−19090.

(7) Xu, B.; Sheibani, E.; Liu, P.; Zhang, J.; Tian, H.; Vlachopoulos, N.; Boschloo, G.; Kloo, L.; Hagfeldt, A.; Sun, L. Carbazole-Based Hole-Transport Materials for Effi cient Solid-State Dye-Sensitized Solar Cells and Perovskite Solar Cells. *Adv. Mater.* **2014**, *26* (38), 6629−6634.

(8) Grisorio, R.; Roose, B.; Colella, S.; Listorti, A.; Suranna, G. P.; Abate, A. Molecular Tailoring of Phenothiazine-Based Hole-Transporting Materials for High-Performing Perovskite Solar Cells. *ACS Energy Lett.* **2017**, *2* (5), 1029−1034.

(9) Zhang, F.; Wang, S.; Zhu, H.; Liu, X.; Liu, H.; Li, X.; Xiao, Y.; Zakeeruddin, S. M.; Grätzel, M. Impact of Peripheral Groups on Phenothiazine-Based Hole-Transporting Materials for Perovskite Solar Cells. *ACS Energy Lett.* **2018**, *3*, 1145−1152.

(10) Saliba, M.; Orlandi, S.; Matsui, T.; Aghazada, S.; Cavazzini, M.; Correa-Baena, J.-P.; Gao, P.; Scopelliti, R.; Mosconi, E.; Dahmen, K.-H.; De Angelis, F.; Abate, A.; Hagfeldt, A.; Pozzi, G.; Graetzel, M.; Nazeeruddin, M. K. A molecularly engineered hole-transporting material for efficient perovskite solar cells. *Nat. Energy.* **2016**, *1* (2), 15017.

(11) Petrus, M. L.; Schlipf, J.; Li, C.; Gujar, T. P.; Giesbrecht, N.; Müller-buschbaum, P.; Thelakkat, M.; Bein, T.; Hüttner, S.; Docampo, P. Capturing the Sun: A Review of the Challenges and Perspectives of Perovskite Solar Cells. *Adv. energy Mater.* **2017**, *7*, 1700264.

(12) Nikiforov, M. P.; Lai, B.; Chen, W.; Chen, Si.; Schaller, R. D.; Strzalka, J.; Maser, J.; Darling, S. B. Detection and role of trace impurities in high-performance organic solar cells. *Energy Environ. Sci.* **2013**, *6*, 1513−1520.

(13) Daskeviciene, M.; Paek, S.; Wang, Z.; Malinauskas, T.; Jokubauskaite, G.; Rakstys, K.; Cho, K. T.; Magomedov, A.; et al. Carbazole-based enamine: Low-cost and efficient hole transporting material for perovskite solar cells. *Nano Energy* **2017**, *32*, 551−557.

(14) Petrus, M. L.; Sirtl, M. T.; Closs, A. C.; Bein, T.; Docampo, P. Hydrazone-based hole transporting material prepared via condensation chemistry as alternative for cross-coupling chemistry for perovskite solar cells. *Mol. Syst. Des. Eng.* **2018**, *3*, 734−740.

(15) Petrus, M. L.; Schutt, K.; Sirtl, M. T.; Hutter, E. M.; Closs, A. C.; Ball, J. M.; Bijleveld, J. C.; Petrozza, A.; Bein, T.; Dingemans, T. J.; Savenije, T. J.; Snaith, H.; Docampo, P. New Generation Hole Transporting Materials for Perovskite Solar Cells: Amide-Based Small-Molecules with Nonconjugated Backbones. *Adv. Energy Mater.* **2018**, *8*, 1801605.

(16) Vaitukaityte, D.; Wang, Z.; Malinauskas, T.; Magomedov, A.; Bubniene, G.; Jankauskas, V.; Getautis, V.; Snaith, H. J. Efficient and Stable Perovskite Solar Cells Using Low-Cost Aniline-Based Enamine Hole-Transporting Materials. *Adv. Mater.* **2018**, *30*, 1803735.

(17) Zhou, W.; Wen, Y.; Ma, L.; Liu, Y.; Zhan, X. Conjugated Polymers of Rylene Diimide and Phenothiazine for n-Channel Organic Field-Effect Transistors. *Macromolecules* **2012**, *45*, 4115−4121.

(18) Maglione, C.; Carella, A.; Centore, R.; Chavez, P.; Leveque, P.; Fall, S.; Leclerc, N. Novel low bandgap phenothiazine functionalized DPP derivatives prepared by direct heteroarylation: Application in bulk heterojunction organic solar cells. *Dyes Pigm.* **2017**, *141*, 169−178.

(19) Salunke, J. K.; Wong, F. L.; Feron, K.; Manzhos, S.; Lo, M. F.; Shinde, D.; Patil, A.; Lee, C. S.; Roy, V. A. L.; Sonar, P.; Wadgaonkar, P. P. Phenothiazine and carbazole substituted pyrene based electroluminescent organic semiconductors for OLED devices. *J. Mater. Chem. C* **2016**, *4*, 1009−1018.

(20) Shinde, D. B.; Salunke, J. K.; Candeias, N. R.; Tinti, F.; Gazzano, M.; Wadgaonkar, P. P.; Priimagi, A.; Camaioni, N.; Vivo, P. Crystallisation-enhanced bulk hole mobility in phenothiazine-based organic semiconductors. *Sci. Rep.* **2017**, *7*, 46268.

(21) Saeki, A.; Koizumi, Y.; Aida, T.; Seki, S. Comprehensive Approach to Intrinsic Charge Carrier Mobility in Conjugated Organic Molecules, Macromolecules, and Supramolecular Architectures. *Acc. Chem. Res.* **2012**, *45* (8), 1193−1202.

(22) Tremblay, M.-H.; Skalski, T.; Gautier, Y.; Pianezzola, G.; Skene, W. G. Investigation of Triphenylamine−Thiophene−Azomethine Derivatives: Toward Understanding Their Electrochromic Behavior. *J. Phys. Chem. C* **2016**, *120*, 9081−9087.

(23) Bolduc, A.; Al Ouahabi, A.; Mallet, C.; Skene, W. G. Insight into the Isoelectronic Character of Azomethines and Vinylenes Using Representative Models: A Spectroscopic and Electrochemical Study. *J. Org. Chem.* **2013**, *78*, 9258−9269.

(24) Karthikeyan, C. S.; Thelakkat, M. Key aspects of individual layers in solid-state dye-sensitized solar cells and novel concepts to improve their performance. *Inorg. Chim. Acta* **2008**, *361*, 635−655.

(25) Bi, D.; Xu, B.; Gao, P.; Sun, L.; Grätzel, M.; Hagfeldt, A. Facile synthesized organic hole transporting material for perovskite solar cell with efficiency of 19.8%. *Nano Energy* **2016**, *23*, 138−144.

(26) Zhang, F.; Liu, X.; Yi, C.; Bi, D.; Luo, J.; Wang, S.; Li, X.; Xiao, Y.; Zakeeruddin, S. M.; Grätzel, M. Dopant-Free Donor (D)−π−

DOI: 10.1021/acsaem.9b00408
ACS Appl. Energy Mater. 2019, 2, 3021−3027

D−π−D Conjugated Hole-Transport Materials for Efficient and Stable Perovskite Solar Cells. *ChemSusChem* **2016**, *9* (18), 2578−2585.
(27) Guo, J. J.; Bai, Z. C.; Meng, X. F.; Sun, M. M.; Song, J. H.; Shen, Z. S.; Ma, N.; Chen, Z. L.; Zhang, F. Novel dopant-free metallophthalocyanines based hole transporting materials for perovskite solar cells: The effect of core metal on photovoltaic performance. *Sol. Energy* **2017**, *155*, 121−129.
(28) Rakstys, K.; Abate, A.; Dar, M. I.; Gao, P.; Jankauskas, V.; Jacopin, G.; Kamarauskas, E.; Kazim, S.; Ahmad, S.; Grätzel, M.; Nazeeruddin, M. K. Triazatruxene-Based Hole Transporting Materials for Highly Efficient Perovskite Solar Cells. *J. Am. Chem. Soc.* **2015**, *137* (51), 16172−16178.
(29) Planells, M.; Abate, A.; Hollman, D. J.; Stranks, S. D.; Bharti, V.; Gaur, J.; Mohanty, D.; Chand, S.; Snaith, H. J.; Robertson, N. Diacetylene bridged triphenylamines as hole transport materials for solid state dye sensitized solar cells. *J. Mater. Chem. A* **2013**, *1*, 6949−6960.
(30) Stolterfoht, M.; Caprioglio, P.; Wolff, C. M.; Márquez, J. A.; Nordmann, J.; Rothhardt, D.; Hörmann, U.; Redinger, A.; Kegelmann, L.; Albrecht, S.; Saliba, M.; Unold, T.; Neher, D. The perovskite/transport layer interfaces dominate non-radiative recombination in efficient perovskite solar cells. 2018, arXiv:1810.01333. *arXiv.org ePrint archive*. http//arxiv.org/abs/1810.01333.

DOI: 10.1021/acsaem.9b00408
ACS Appl. Energy Mater. 2019, 2, 3021−3027